Methods for Accurate Acoustic Characterization with Ultra-Low Noise and Minimal Effect from Acoustic Reflections

Junpeng Lai, Morteza Karimi, and Ronald N. Miles[*]

Department of Mechanical Engineering, Binghamton University, Binghamton, NY 13902

jlai16@binghamton.edu; miles@binghamton.edu

Abstract

It is common to measure the response of devices and structures to sound due to an imposed sound source. Unfortunately, acoustic reflections from walls and/or instruments often contaminate the results. In this paper, methods of acoustic characterization are described to minimize the influence of acoustic reflections. It is shown that this process results in clean and smooth data. A simple time-domain window is implemented for diminishing the contribution from reflection waves. Moreover, a single frequency curve fitting approach is employed for better parameter identification and noise reduction, compared to traditional fast Fourier Transform analysis. Results obtained from a theoretical acoustic model with a reflection source are compared with measured results. Different cases of data acquisition with time and frequency analysis are experimentally demonstrated and validated. All experimental measurements are performed in an anechoic chamber. Results show that the approach presented here significantly reduces noise and also the influences of reflection waves in experimental data acquisition outcomes.

1 Introduction

A traveling sound wave is often described by fluctuations of sound pressure and media particle velocity over space and time. Acoustic sensors are designed to detect these fluctuations. As a crucial process of sensor design, acoustic characterization often refers to the measurements of the values of sounds and noises in terms of their intensities and various quantitative features including their spectra or the growth and decay of the sound over time [1-3]. During most characterizations, the principal values measured in acoustics are usually sound pressure, and sound induced velocity, which are important characteristics of sound in order to have a complete and exact prediction of sound behaviors [4-6]. For sound pressure measurements a standard microphone is often used by transducing the received acoustic signals (pressures) into proportional electrical voltages for readout. For acoustic induced vibration velocity, a laser vibrometer is often utilized in which the received signals (velocity) are transduced to proportional electrical voltages [7,8]. The difficulties experienced in acoustic measurements are due to the complicated spatial distribution of the acoustic values in rooms as well as the variability of sounds and noises over time. Electro-magnetic noise and acoustic noise is another main contributor as it can contaminate the incident sound wave and final data. Sound wave reflection occurs when sound waves (incident wave) leave one medium and enter another, with a portion of the wave passing through the medium, while the remainder of the wave reflecting back. The reflected wave will either sum up or cancel out with the incident wave, and thus greatly skew the expected results [9,10]. The anechoic chamber can greatly reduce the effect of the acoustic noise and sound wave reflections, which we shall discuss more later in the paper. Electromagnetic noise, especially inside the chamber, cannot be easily eliminate. Acoustic

measurements are closely associated with electrical measurements and are performed chiefly with electronic measuring instruments. All of which could be sources of electromagnetic noise that may impact nearby devices and pollute the data with associated frequency noise. The approach presented in the following is intended to minimize the influence of both unwanted noise and acoustic reflections.

To reduce acoustic reflections, it is common to employ conventional sound-absorbent foams and fibers that are used to cover reflecting surfaces [11-15]. Liao et al. [16] introduced novel adaptive metamaterials for broadband sound absorption at low frequencies, which are typically very difficult to attenuate passively. It has been shown that the absorption coefficient of the adaptive metamaterial can be greater than 0.9 in the frequency region, 112–236 Hz. Shen et al. [17] studied hierarchical pore structure based on cellulose nanofiber/melamine composite foam to enhanced sound absorption performance. The sound absorption coefficient of the composite foam has an improvement of 80 %.

Noise reduction in acoustic measurement characterization has remained a primary research interest for decades. The very first techniques used for denoising the acoustic signals are use of analog or digital filters [18]. These filters have a simple structure and are easy to implement but cannot provide significant distinction between signal and noise. Excellent denoising algorithms have been developed. For instance, Boashash and Mesbah [19] used time-frequency peak filtering (TFPF) to enhance signal on both simulated and real data. Moreover, Xiang and Yan [20] proposed a new time-frequency analysis method, called self-adaptive Wigner-Ville distribution based on local mean decomposition, to effectively analyze non-stationary amplitude-modulated and frequency-modulated signals. They showed that the proposed model could analyze the multi-component signal with multiple frequency components, and evidently remove

the cross-terms of Wigner-Ville distribution, and keep all its advantages. In addition, a noise reduction technique for acoustic-based systems was proposed based on Empirical Mode Decomposition (EMD) and improved fruit fly optimization algorithm (IFFOA) [21]. The validity of the noise reduction technique was verified by simulation and an actual acoustic-based diagnosis system. Based on simulations and comparison results, they demonstrated that the automatic denoising method could effectively eliminate noise and outperform the others. Fast Fourier Transform (FFT) is the most widely used technique in signal analysis [22].

Noise and reflection reduction are significant problems in diverse areas and applications in acoustic measurements. The development of methods for minimizing these effects is ongoing. In this paper, we will show that even with the use of a highly-absorbent anechoic chamber, there can still be detectable reflection from the walls and/or the equipment, that can contaminate the results of measurements. In the following, we describe a process that successfully eliminates the effect of reflections and unwanted noise when performing acoustic measurements.

2   Methods

All experiments are conducted in the anechoic chamber at Binghamton University, shown in figure 1. The chamber interior dimensions are 4.2 m wide, 5.4 m long, and 3.2 m tall. The absorbent wedges shown are made of fiberglass. The chamber has been certified by the manufacturer to provide an anechoic environment at all frequencies above 80 Hz. The anechoic chamber was tested using methods specified in: ISO Standard 3745-2003, Annex A, "General procedures for qualification of anechoic and hemi-anechoic rooms".

Fig. 1 Anechoic chamber at Binghamton University

Figure 2a shows a plan view of the anechoic chamber. Figure 2b shows the experimental setup and system diagram. Here, sound pressure is measured by a B&K Type 4138 1/8" reference microphone and amplified by a B&K dual microphone power supply Type 5935L. A Polytec OFV-534 laser vibrometer is used for measuring the velocity of various test samples. The laser beam can be maneuvered by a set of motorized stages. The signal of the microphone and the

laser vibrometer are collected by a National Instruments PXI 1033 data acquisition system. The stimulus signal is generated by MATLAB and sent through the data acquisition system. After the crossover filter dbx Model 234xs, the signal is divided to low frequency, mid-range frequency, and high frequency, amplified by Crown D-75and Techron 5530, and sent to the woofer, midrange, and tweeter, respectively. The loudspeaker is placed 3 *m* away from the microphone location.

(a)
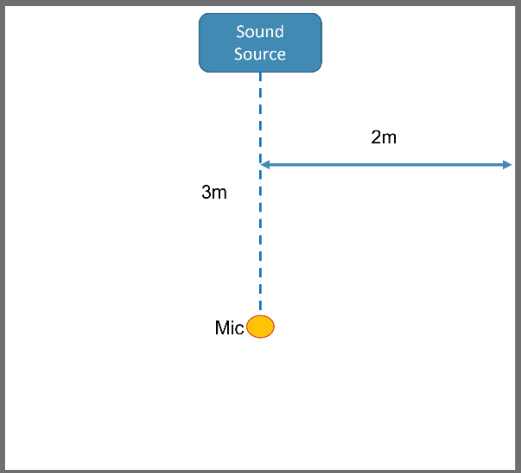
(b)
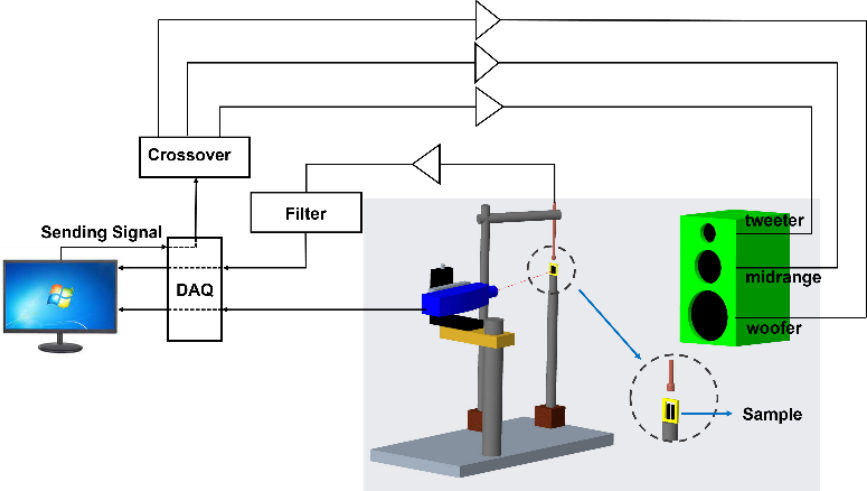
Fig. 2 (a) Top-down Chamber diagram. The speaker is located 3m away from the reference microphone for approximate plane sound wave. The side wall of the chamber is 2m away from the center line of the experimental setup. (b) Detailed experimental setup and system diagram.

A complete description of a sound field requires both the sound pressure p (r, t) and the medium particle velocity vector u (r, t), where r the spatial vector, t is time. The pressure may be taken as proportional to density variations, while the velocity vector describes the velocity of disturbance of the physical particles in the medium. The definition of a plane wave requires a wave that only propagates in one direction in a cartesian coordinate system and has a velocity fluctuation direction that is parallel to the propagation direction. In such wave, the acoustic pressure and velocity are uniform anywhere across the fluctuation plane.

It's possible to show the wave generated can be considered as a plane wave. If we consider the loud speaker is generating a harmonic spherical wave that propagates in the radial direction r, the wave equation has the solution form of [23]:

$$P(r,t) = \frac{A}{r}e^{i(\omega t - kr)} \tag{2.0.1}$$

Where A is a constant, r is the radius of the sphere wave, $k = \frac{\omega}{c}$ is the wave number. Using the Euler equation, the velocity can be calculated:

$$U(r,t) = \frac{A}{r}e^{i(\omega t - kr)}\frac{1}{\rho_0 c}\left(1 + \frac{1}{ikr}\right) \tag{2.0.2}$$

For a plane wave:

$$\frac{P(x,t)}{U(r,t)} = \frac{1}{\rho_0 c} \tag{2.0.3}$$

For the spherical wave, the relation between $P(r,t)$ and $U(r,t)$ can be written as:

7

$$\frac{P(x,t)}{U(r,t)} = \frac{1}{\rho_0 c}\left(\frac{ikr}{1+ikr}\right) \tag{2.0.4}$$

To consider the wave as a plane wave at measured location, we need $kr \gg 1$. That is:

$$r \gg \frac{\lambda}{2\pi} \tag{2.0.5}$$

Where λ is wave length of the sound wave. If the distance is larger than a wave length

$r \geq \lambda$, we should be able to consider $P(x,t) = \frac{1}{\rho_0 c}U(r,t)$.

Thus, for the acoustic measurement setup shown in figure 2, the sound wave can be considered

as plane wave above 100Hz.

2.1 Effect of reflections in an anechoic chamber

Figure 3 shows measured sound pressure levels (SPL) obtained in the chamber using the setup

described in figures 1 and 2. A constant amplitude swept sinusoidal signal from 100Hz to

10kHz is played through the loudspeaker as the stimulation. The predicted and measured results

show a significant, fluctuation in SPL that appears to be periodic in frequency. Note that the

frequency axis has a logarithmic scale.
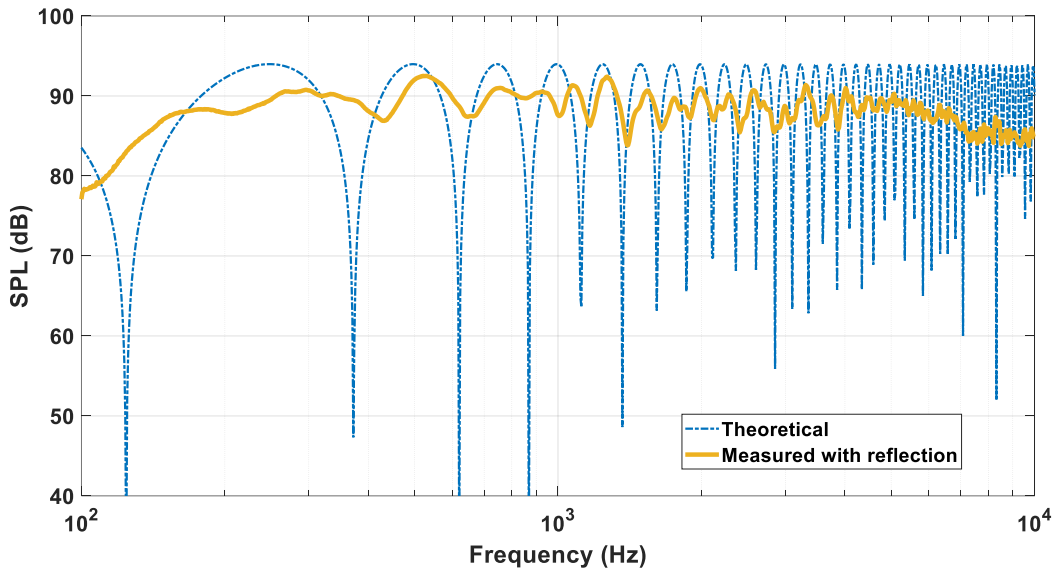
Fig. 3 Reflections cause fluctuations in measured sound pressure levels. The sound output of the source is constant in frequency but the measured sound pressure level varies significantly as a function of frequency. The dashed line shows sound pressure level (SPL) predicted for a frequency independent sound source with a single mirror reflection source model according to the dimensions of the chamber. The solid line shows the measured SPL with the effect of the reflection wave.

Anechoic chambers are typically designed to minimize ambient noise, and more importantly, absorb internal reflection sound waves during an acoustic characterization involving sound generation. However, the result shown in Fig. 3 shows that even in a state-of-the-art anechoic chamber, there are still reflection waves which are not fully attenuated. The data influenced by reflections will show a frequency dependent response with peaks and dips, caused by the reflection wave. Specifically, around 1500Hz, the sound pressure level (SPL) variation is over 10dB, which means the difference of sound pressure in pascals will be over 330 percent. The main cause of this issue is that although anechoic chambers have extremely absorbent walls compared to a normal wall, it cannot absorb all incident sound waves. That little amount of

reflection is usually neglected. But, unfortunately, a small contribution from a reflected wave can have a significant influence on the total sound field.

It is worthwhile to briefly consider a highly simplified system in which we can readily account for reflections from absorbing surfaces to see how the variations in pressure across frequency depend on the absorption of the surface. When a sound field consists of the combination of an incident and reflected wave, the pressure can be expressed as:

$$P(x,t) = e^{i\omega t}\left(P_1 e^{-ikx} + P_2 e^{ikx}\right) \tag{2.1.1}$$

where p_1 and p_2 are the complex amplitudes of the incident and reflected waves, respectively and the wave number is $k=\omega/c$. ω is frequency in *rad/s* and c is the sound speed. The sound pressure at a distance l to the left of the reflecting surface, may be computed from Eq. (2.1.1), at $x=-l$,

$$P(-l,t) = e^{i\omega t} P_1 e^{ikl}\left(1 + re^{-2ikl}\right) \tag{2.1.2}$$

where $r=p_2/p_1$ is called reflection coefficient. The mean square pressure can be determined as follows:

$$<P^2> = \frac{\Re[P(-l,t)P^*(-l,t)]}{2} = \frac{|P_1|^2}{2}\left(1 + re^{-2ikl}\right)\left(1 + r^* e^{2ikl}\right)$$

$$= \frac{|P_1|^2}{2}\left(1 + 2\Re[re^{-2ikl}] + |r|^2\right) \tag{2.1.3}$$

where $\Re[\cdot]$ denotes the real part and the superscript * denotes the complex conjugate.

We will assume that the reflecting surface is relatively absorbent so that $r<<1$. Neglecting $|r|^2$ in Eq. (2.1.3) gives

$$< P^2 > \approx \frac{|P_1|^2}{2}(1 + 2rcos(2kl)) \qquad (2.1.4)$$

Sound pressure level (SPL) can be express as follows:

$$SPL = 10 \, log_{10}(\frac{< P^2 >}{P_{ref}^2}) \qquad (2.1.5)$$

where $P_{ref}=20\times10^{-6}$ pascal is the standard reference pressure. Substituting Eq. (2.1.4) into Eq.

(2.1.5), Sound pressure level will give [23]

$$SPL = 10 \, log_{10}\left(\frac{|P_1|^2(1 + 2rcos(2kl))}{2P_{ref}^2}\right)$$

$$= 10 \, log_{10}\left(\frac{|P_1|^2}{2P_{ref}^2}\right) + 10 \, log_{10}(1 + 2rcos(2kl)) \qquad (2.1.6)$$

The sound absorption coefficient may be written as:

$$\alpha = 1 - \left|\frac{P_2}{P_1}\right|^2 = 1 - r^2 \qquad (2.1.7)$$

It can be seen that by decreasing the absorption coefficient, the sound pressure variation

increases dramatically. To be specific, if the absorption coefficient is α =0.9, the sound pressure

level fluctuation is calculated to be SPL=+-2.75dB. That means that when viewed as a function

of frequency, the fluctuating maximum sound pressure in pascals will be approximately twice the

value of the minimum.

In the calculated results shown in figure 4, different absorption coefficients are applied, and the corresponding sound pressure levels are calculated over frequency for a highly simplified one-dimensional (1D) sound field. It shows the effects of different sound absorption coefficient α, on SPL for various frequencies.
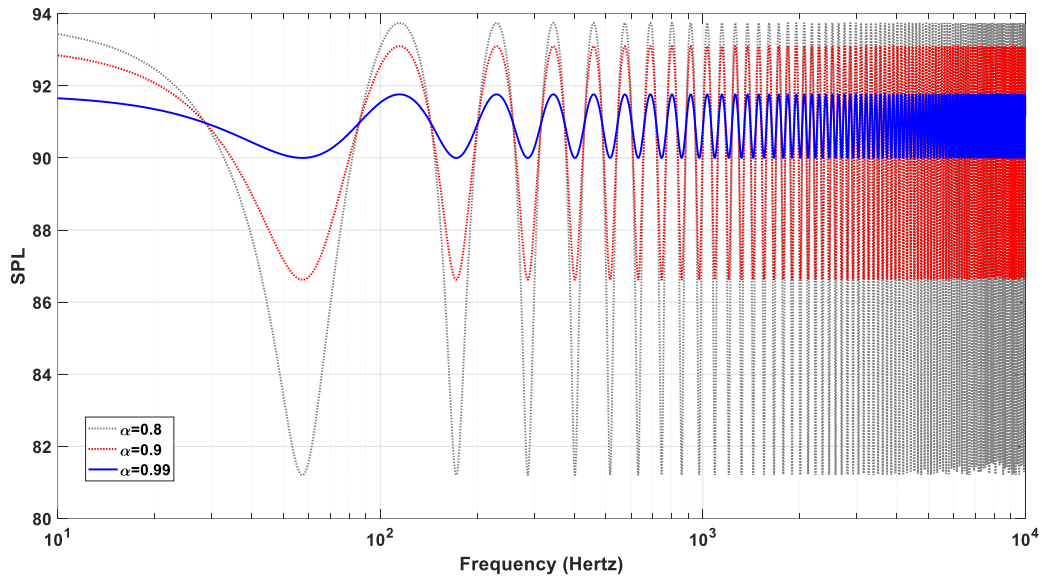
Fig. 4 Variations of SPL versus frequencies for different absorption coefficients

Moreover, the presence of the equipment and experimental setups will further increase the reflection which will create periodic, variations in the results when viewed in the frequency domain.

To solve this problem, one can reduce the reflection wave by increasing the absorption ratio for the reflected surfaces, in this case, the chamber walls, which is not practical since there is little room to improve the wedges to be more absorbent. That is why a more general method is

adopted to get rid of the reflection wave effect. A time domain window method is introduced as an effective way to 'filter' out the unwanted reflection wave.

Before demonstrating the details of the method, consider a simplified example for analyzing the time domain signal with a reflection wave, as indicated in figure 5a. A flat surface is added to the setup 36.5cm away behind the reference microphone. By creating a solid wall of reflection on the path of sound wave propagation, we can analyze the timing of the reflection wave and its interaction with the incident wave. A single frequency signal at 500Hz is generated by the speaker 3m away from the microphone. The time domain response of the acoustic pressure fluctuation collected by the microphone is shown in figure 5b. The signal acquired by the microphone is divided to 4 parts. Before the time 'tstart' is when sound wave hasn't travelled to the microphone diaphragm, where tstart is the time when the sound wave reaches the microphone. Transient response is acquired in the time period soon after tstart. As the sound wave travels to the wall behind the microphone, reaches the wall, and reflects back, the microphone signal in this period is completely reflection free. After the reflection wave arrives at the microphone again, the reflection wave interacts with the incident wave. The predicted time at which the reflected wave first arrives at the microphone can be expressed as:

$$t\_reflection = tstart + 2*d/c \qquad\qquad (2.1.8)$$

where c is the speed of sound at room temperature, 344 *m/s,* and d is the distance between the microphone and the reflecting surface, which can be verified by calculating d from Eq. (2.1.8) using measured time domain data. To avoid the effect of the reflection wave, the analysis should be cast within the reflection free section. Using the experiment setup shows in Fig. 5, the times shown in Fig. 6 are identified on the plot of the measured data. A manual identification process

is added to start the analysis of the data after the transient response died out, and stop the analysis before the reflection wave arrives. This way, the data analyzed will not be contaminated by the speaker transient response or the interaction with the reflection wave.
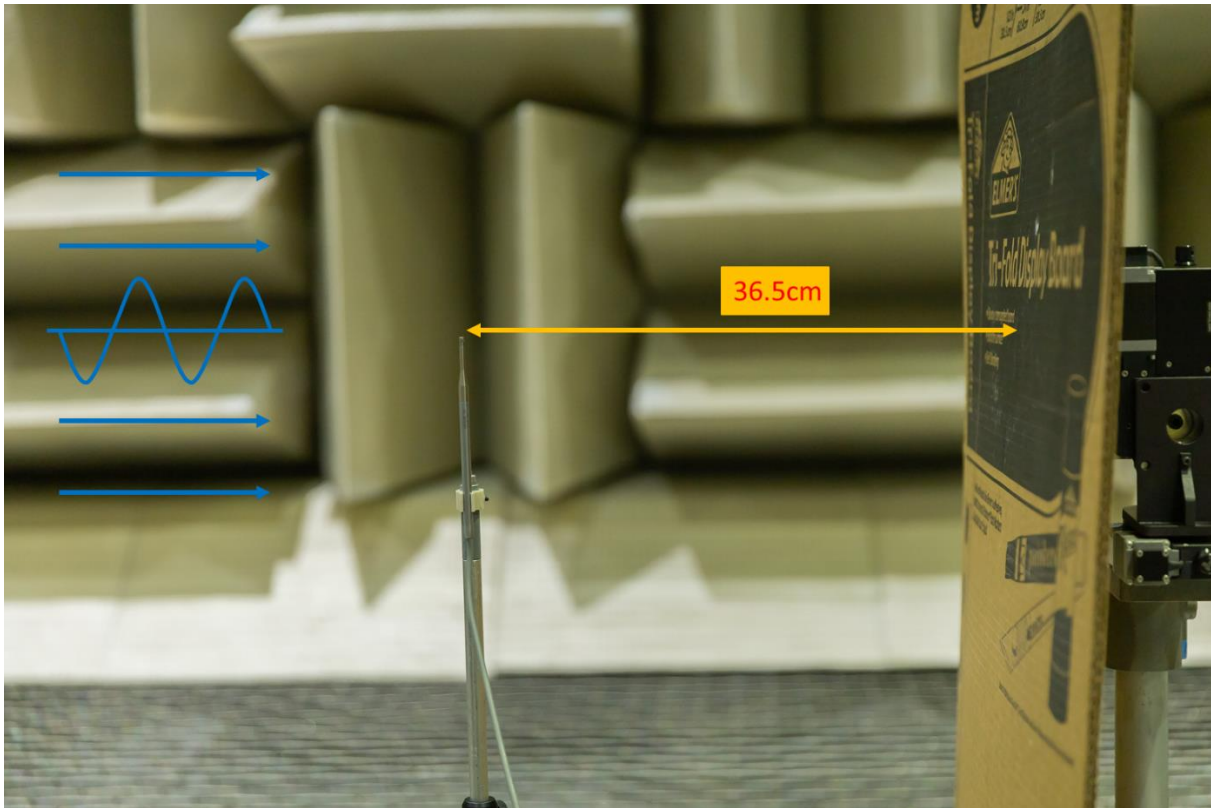
Fig. 5 Experiment setup for analyzing reflection wave. A simple reflection case is created to analyze the time domain signal. Single frequency plane sound wave is sent through speaker from 3m away from the reference microphone. A solid vertical wall is 36.5cm behind the microphone.
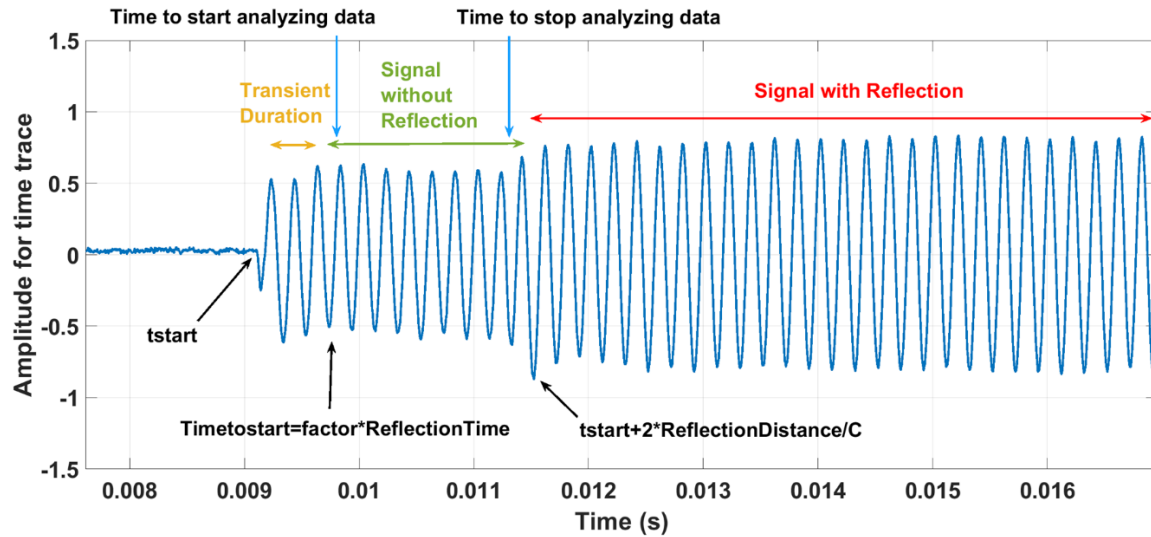
Fig. 6 Time domain pressure acquired by the microphone. The sound arrives at the microphone at time tstart. The transient response of the sound source then influences the signal for a time, TransientDuration. After the transient has died out, the signal is analyzed until the reflected wave arrives.

2.2 Noise rejection and reflection windowing

Measuring the acoustic frequency response is a significant process for characterizing structures and acoustical devices. Typical ways include using broadband white noise or swept sinusoidal signals as sound stimuli, analyze the measured signal using fast Fourier Transform to process the data and acquire broadband frequency response. Through the use of the FFT, the acquired signal data is weighted in the frequency domain.

In our case, using random broadband signals means the sound power generated by the loudspeaker is spread to all the frequencies involved. Instead, we can send just one frequency at a time; all available sound power can be concentrated at this single tone. This way, the system doesn't need to be driven at all frequencies at the same time. All available energy can be focused

15

to increase the sound power at the targeted frequency, which will result in a higher signal to noise ratio, thus cleaner data. Another benefit of sending one frequency tone at a time is that it facilitates the creation of a time-domain analysis window as depicted in Fig 6. By sending out just one frequency, the duration of the pure tone can be actively controlled. Since we know the reflection wave will arrive at some point, the microphone recording needs to be shut off before that. By adjusting the time range when the microphone is listening to the signal, we created a time window in which we are receiving the signal, and shut off and stop receiving the reflection contaminated signal. For lower frequencies, a specific number of cycles are used to compensate the long wavelength. Because the acquired signal contains only one frequency component, a curve fitting process is used to analyze the data with better accuracy, especially for lower frequencies.

The effective reflections in an anechoic chamber can be very difficult to eliminate. However, using pure tone signals with a dedicated time window, the reflection can be eliminated. To attenuate the effective noise, a narrow band least square curve fitting process has been used [23].
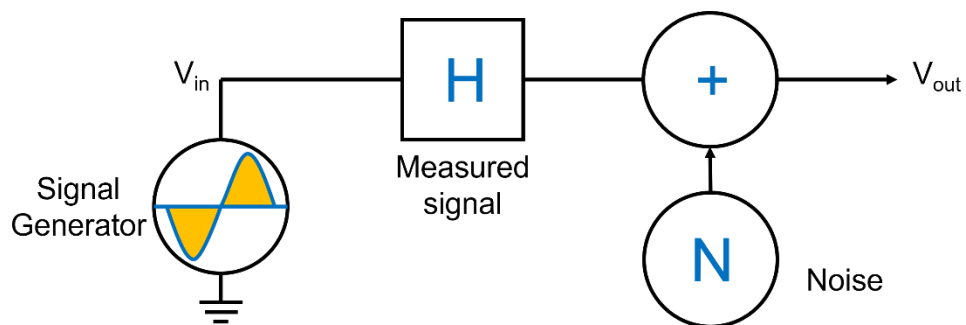
Fig. 7 Signal acquisition process. A series of sinusoidal signals are generated. The actual measured signal at each frequency is always combined with noise during the measurement.

Assuming there is a sinusoidal signal generated by the signal generator, the voltage is denoted as V_{in},

$$V_{in} = V_0 \sin(\omega t) \tag{2.2.1}$$

where ω is the known driving frequency. The signal has been through the data acquisition process, and noise has been introduced during the process. Possible noise sources include electronic noise due to ground loops, random thermal noise, environmental acoustic noise, etc. V_{out} is the signal acquired by the data acquisition system.

$$V_{out} = V_0 \sin(\omega t + \varphi) + N(t) \tag{2.2.2}$$

Where φ is the phase shift due to the room dynamics or structure effect during the measurement process. $N(t)$ is the introduced effective noise. If we account for DC shift in the process, the desired response without noise V_o can be assumed to be:

$$V_o = a \cos(\omega t) + b \sin(\omega t) + c \tag{2.2.3}$$

Where a, b, and c are constants to be found. Since the measured time data is discrete, t is replaced as t_i, where $i = 1, 2, \cdots, N$, is the number of data points. Thus, Eq. (2.2.3) can be rewritten as follows:

$$V_{oi}(t_i) = a \cos(\omega t_i) + b \sin(\omega t_i) + c \tag{2.2.4}$$

To curve fit the measured data, different sets of parameter a, b, c will be found to ensure V_{oi} can represent the data as well as possible. The error at each t_i is

$$\epsilon_i = a \cos(\omega t_i) + b \sin(\omega t_i) + c - V_{oi}(t_i) \tag{2.2.5}$$

17

There are N equations and 3 unknowns. By solving the overdetermined system for a, b, and c, the optimum V_{oi} can be found to represent the data. Simply assume ϵ_i to be 0, Eq. (2.2.5) can be written as:

$$\begin{bmatrix} \cos(\omega t_1) & \sin(\omega t_1) & 1 \\ \cos(\omega t_2) & \sin(\omega t_2) & 1 \\ \cos(\omega t_3) & \sin(\omega t_3) & 1 \\ \vdots & \vdots & \vdots \\ \cos(\omega t_N) & \sin(\omega t_N) & 1 \end{bmatrix}_{N \times 3} \begin{pmatrix} a \\ b \\ c \end{pmatrix}_{3 \times 1} = \begin{pmatrix} V_{o1} \\ V_{o2} \\ V_{o3} \\ \vdots \\ V_{oN} \end{pmatrix}_{N \times 1} \qquad (2.2.6)$$

Solve Eq. (2.2.6) for a, b, c. The curve fitted signal amplitude is

$$A = \sqrt{a^2 + b^2} \qquad (2.2.7)$$

Phase with respect to the signal origin is

$$\varphi = \tan^{-1} \frac{b}{a} \qquad (2.2.8)$$

The added narrow band curve fitting process uses least squares to minimize the fitting error. The fitted signal should be the closest representation of the measured data. Since the acoustic signal is carefully sent, the frequency to expect for curve fitting is known. It is highly unlikely for the curve fitting process to be confused with noise at other frequencies. Therefore, the effective noise has been greatly attenuated.

3   Results and discussions

3.1   Acoustic pressure

As presented above, when measuring sound pressure alone, reflection from the anechoic chamber wall will contaminate the result. With the time-domain window rejecting the reflection

wave, and narrow band curve fitting filtering the noise which has been shown in Fig 5 (a) and

(b), respectively, a clean and smooth frequency response can be achieved as shown in Fig. 8(a).

(a)
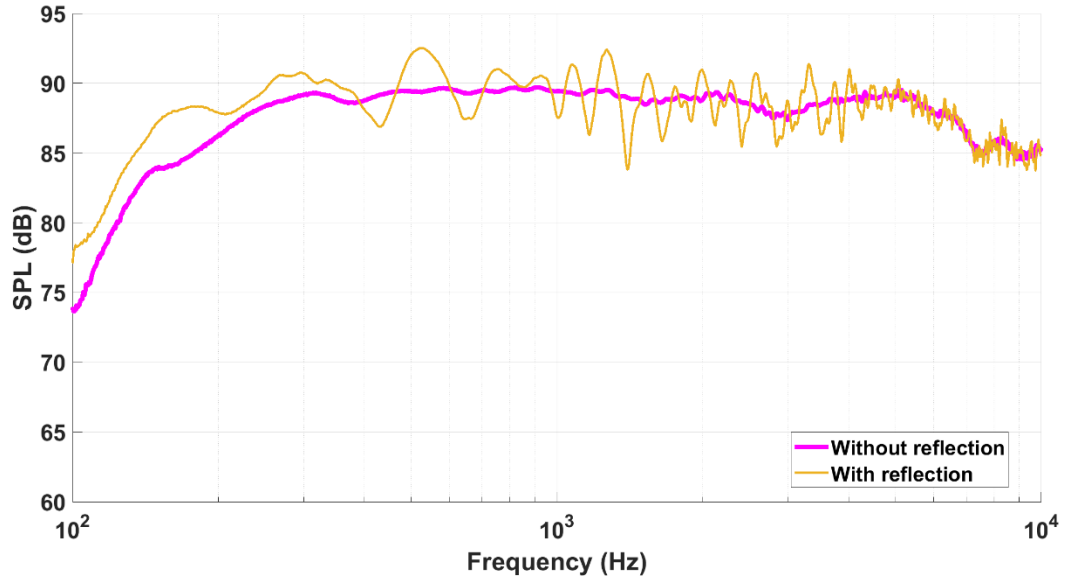
(b)
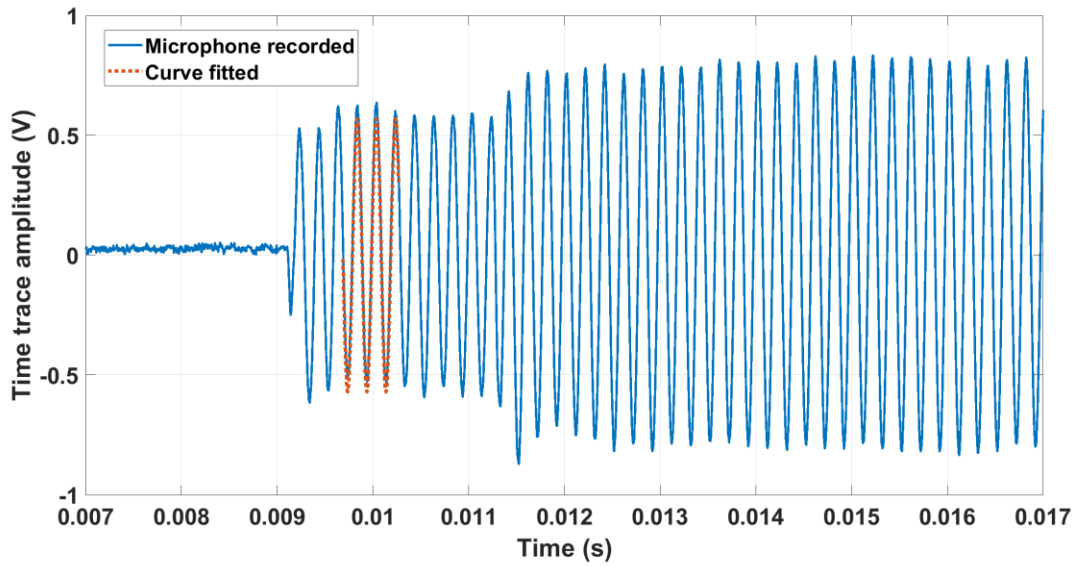
Fig. 8 The time domain window leads to smoother measured data when plotted in the frequency domain. (a) Frequency domain data before and after elimination of reflection. The reflections within the anechoic chamber cause significant fluctuation in the data when plotted versus frequency. (b) Time domain data obtained at a particular frequency and the results of windowing and curve fitting to filter out measurement noise.

As shown in Fig. 8, the method is extremely effective at removing the effect of the reflection wave. The signal local variation as a function of frequency is reduced from 12dB to less than 3dB after the reflection is removed. The time domain data shows the time interval before and after the reflection wave arrives at the microphone and the data used in the curve fitting process. Since the reflection wave arrived after the data used in the curve fit, the results are not influenced by reflections.

3.2 Sound induced velocity

Another example of taking advantage of this method is when measuring the acoustic induced velocity. The experimental setup used is the same as shown in figure 2, with the addition of an extremely thin fiber suspended in the sound field that is used to estimate the acoustic particle velocity [24,25]. The fiber used consists of spider silk that is placed adjacent to the reference microphone. We have shown that the spider silk can provide an accurate means of measuring the acoustic particle velocity. The sound-induced velocity of the silk is measured using a laser vibrometer. The laser is pointing at the silk strand from 29 *cm* away. The silk strand is simply supported by two thin pins with minimal internal tensile stress. Based on our previously published result [24,25], the velocity frequency response of the spider silk is nearly independent of frequency and close to that of the surrounding air particle velocity. With the reflection from

20

the already absorptive chamber wall removed using the previously introduced method, the measured velocity frequency response is found to be nearly independent of frequency. Since at the measured location, the sound wave can be considered as a uniform free field plane wave, the acoustic air particle velocity nearby the measured location $u(t)$ has a linear relationship with the measured acoustic pressure $p(t)$ and can be determined by:

$$u(t) = p(t)/\rho_0 c \qquad (3.2.1)$$

where ρ_0 is the density of air, c is the speed of sound in air. The velocity of the silk sample can be measured by the laser doppler vibrometer. All measured time signals are processed with least square curve fitting thus most acoustical, electronic and electromagnetic noise can be avoided when analyzing the signals in the frequency domain. This way, the acquired data should be free of contamination from the reflection and noise. As shown in figure 8 (a), (b), the velocity of the silk is closely representing the expected acoustic particle velocity of the air. The method used here is similar to the method used when measuring the acoustic motion of the spider orb-web experiment [25].

(a)
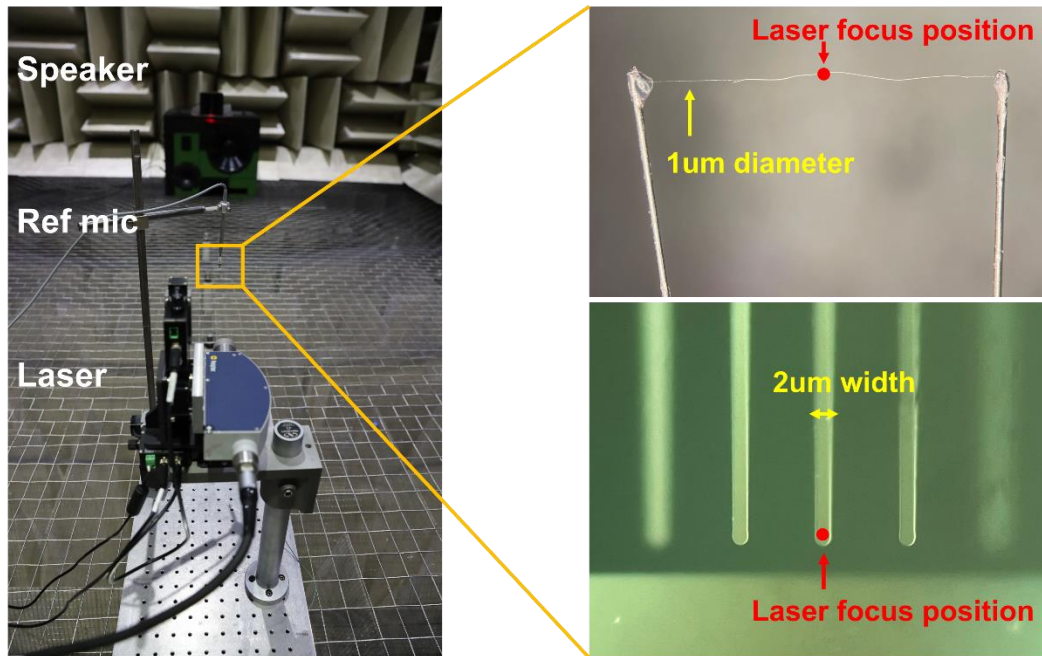
(b)
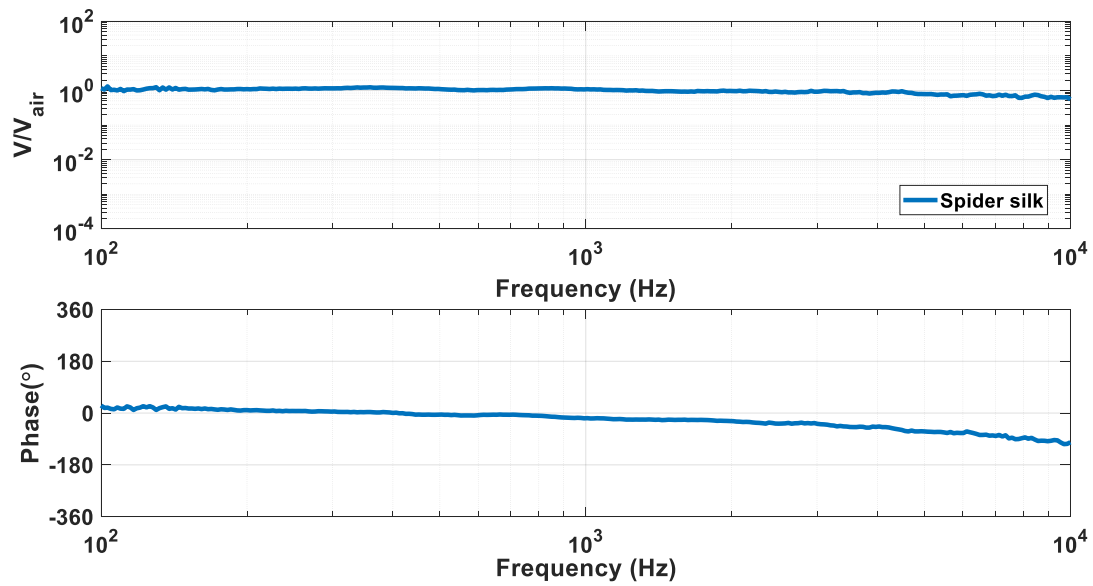
Fig. 9 Measurement of the acoustic induced velocity using the method. (a) Acoustic setup of

the measurement and detailed photo of the measured sample. The speaker is 3m away from the

measured location. The reference mic is set adjacent to the object measured. Laser vibrometer

measuring velocity on the sample. The first sample is a strand of tension free spider silk drag line. The second sample is a silicon based compliant cantilever beam. The setup is used to acquire data for Fig. 9(b) and Fig. 10. (b) Measured velocity response to plane wave sound across the frequency range of 100Hz to 10kHz.

Having a good measure of the acoustic particle velocity is useful in many situations. If a structure can move closely with the air, it can be calibrated for velocity sensing during acoustic characterizations. Spider silk can be difficult to handle and contains too much random variables during the fabrication process, whereas a microfabricated silicon cantilever beam that is thin enough to move with the air is better suited as a reliable velocity probe. The calibration process is similar to measuring the velocity of the silk. However, the velocity frequency response of a cantilever beam is more frequency dependent than a compliant strand of silk. To represent the velocity of the air particles due to a sound wave, velocity compensation should be considered in low frequencies.

The calibration of the sensing beam velocity sensitivity is expressed in terms of the transfer function between the measured beam velocity and air particle velocity. Thus, the measured transfer function H_1 is:

$$H_1 = \frac{V_{beam\_cali}}{V_{air\_cali}}$$

(3.2.2)

Where V_{beam_cali} is the velocity measured with the laser vibrometer during the calibration process, and V_{air_cali} is the air particle velocity in a plane wave. When performing an air particle velocity measurement, the micro beam is placed at the desired location with the laser focused on the beam. The measured air particle velocity can be calculated as:

23

$$V_{air} = V_{beam}/H_1 = V_{beam} \cdot \frac{V_{air\_cali}}{V_{beam\_cali}} \tag{3.2.3}$$

WhereV_{air} is the air particle velocity at the location under investigation, V_{beam} is the

corresponding beam velocity response measured by the laser vibrometer. As shown in figure 9.
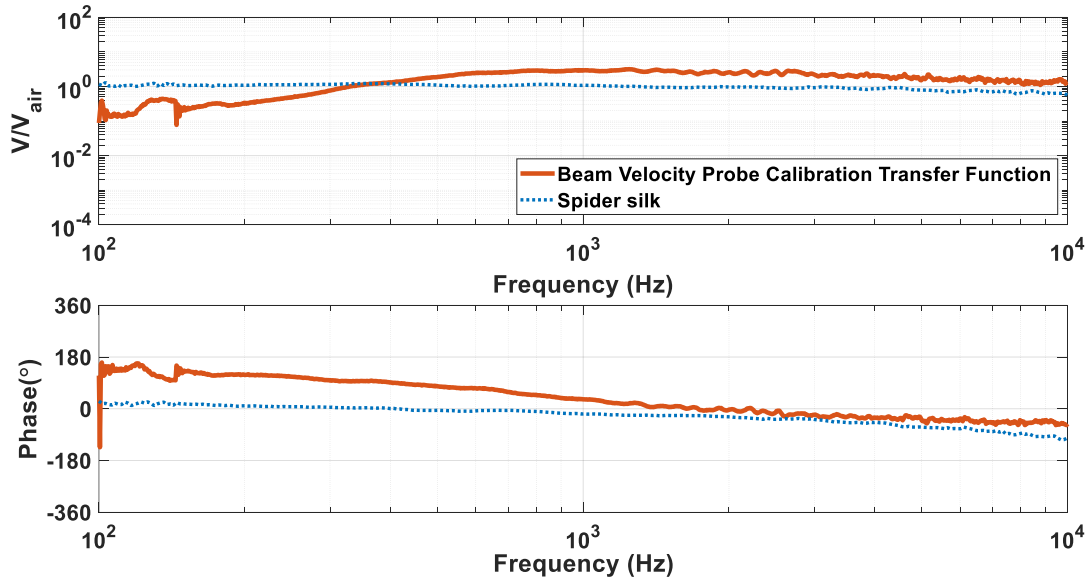
Fig. 10 Measured velocity of the silicon beam response to plane wave sound compared with

spider silk response. The solid line is measured velocity of the beam. The dotted line is the

velocity measured from Fig. 9 (b). Getting rid of the reflection helps to get a clean velocity

measurement.

4   Conclusion

It is often preferred to perform an acoustic response measurement in an anechoic chamber due to

its performance like ultra-low noise, minimal air flow, and minimal influence from acoustic

reflections. Although when attempting to detect faint fluctuations of acoustic pressure or trying

to measure acoustic particle velocity, the resulting data are sensitive to low levels reflections

such as those from the chamber wall or the equipment in the experimental setup. The consequences are considerable frequency dependent variations in the final frequency response. These variations are misleading at times, and thus need to be eliminated. A time-domain window incorporated with human interactions was created to help modify the data acquisition process in order to control the imposed sound and signal receiving duration. Instead of physically removing the reflection source, since it is not always feasible, it filtered the effect of the reflection from the measured data. And since the imposed pure tone is used as a sound source, it is easier to employ narrow band least squares to fit the data for every section of the sent tone for different frequencies, in which process the noise from all other irrelevant frequencies is filtered out. Results showed the smoothness of data comparing before and after the method was applied. After getting rid of the reflection and noise, the data variation across the wide frequency band from 100Hz to 10kHz has dropped from 12dB to less than 3dB, shown in Fig. 8(a). Since the sound wave can be considered as a uniform plane wave, a better pressure measurement leads to a more accurate measure of air particle velocity. This can be helpful when characterizing the response of a structure that is intended to be driven by air particle velocity.

This method offered an approach to characterize the sound pressure as well as the media particle velocity without being affected by reflection wave and noise. The time-domain approach described here can be an effective alternative to frequency-domain analyses that employ the FFT algorithm. Not all acoustic characterization can be done in an anechoic chamber and acoustic reflections can have an adverse effect on the measured results. We showed that even if the experiment is conducted in an anechoic chamber, there could still be reflections from the walls that significantly impact the results. The approach presented here can lead to clean results with the measurement conducted in a relatively quiet conventional room without anechoic surfaces.

5   References

[1]   Rienstra, S. W., & Hirschberg, A. (2004). An introduction to acoustics. Eindhoven University of Technology, 18, 19.

[2]   Salomons, E. M. (2001). Computational atmospheric acoustics. Springer Science & Business Media.

[3]   Maling Jr., G.C. (2014). Noise. In: Rossing, T.D. (eds) Springer Handbook of Acoustics. Springer Handbooks. Springer, New York, NY.

[4]   Davies, P. O. A. L. (1988). Practical flow duct acoustics. Journal of Sound and Vibration, 124(1), 91-115.

[5]   Rossing, T. D., & Fletcher, N. H. (2004). Principles of vibration and sound. The Journal of the Acoustical Society of America, 116, 2708

[6]   Kadam, V.V., Nayak, R. (2016). Basics of Acoustic Science. In: Padhye, R., Nayak, R. (eds) Acoustic Textiles. Textile Science and Clothing Technology. Springer, Singapore.

[7]   Purohit, A., Darpe, A. K., & Singh, S. P. (2016). Experimental investigations on flow induced vibration of an externally excited flexible plate. Journal of Sound and Vibration, 371, 237-251.

[8]   Chen, S., Fatemi, M., & Greenleaf, J. F. (2002). Remote measurement of material properties from radiation force induced vibration of an embedded sphere. The Journal of the Acoustical Society of America, 112(3), 884-889.

[9]   Zhu, H., Rajamani, R., & Stelson, K. A. (2003). Active control of acoustic reflection, absorption, and transmission using thin panel speakers. The Journal of the Acoustical Society of America, 113(2), 852-870.

[10]   Krasil'nikov, V. A., & Krylov, V. V. (1984). Introduction to physical acoustics.

[11]   Sagartzazu, X., Hervella-Nieto, L. & Pagalday, J.M. (2008). Review in Sound Absorbing Materials. Arch Computat Methods Eng 15, 311–342.

[12]   Gao, N., Tang, L., Deng, J., Lu, K., Hou, H., & Chen, K. (2021). Design, fabrication and sound absorption test of composite porous metamaterial with embedding I-plates into porous polyurethane sponge. Applied Acoustics, 175, 107845.

[13]   Bujoreanu, C., Nedeff, F., Benchea, M., & Agop, M. (2017). Experimental and theoretical considerations on sound absorption performance of waste materials including the effect of backing plates. Applied Acoustics, 119, 88-93.

[14]   Zhu, H., Rajamani, R., & Stelson, K.A., (2003). Active control of acoustic reflection, absorption, and transmission using thin panel speakers", The Journal of the Acoustical Society of America,113, 852-870

[15]   Ma, X., Chen, K., Wang, L., Liu, Y., & Ding, S. (2022). Active control of low frequency sound absorption of large sized micro-perforated panel absorber by using point source. Applied Acoustics, 185, 108424.

[16]   Liao, Y., Zhou, X., Chen, Y., & Huang, G. (2018). Adaptive metamaterials for broadband sound absorption at low frequencies. Smart Materials and Structures, 28(2), 025005.

[17]   Shen, L., Zhang, H., Lei, Y., Chen, Y., Liang, M., & Zou, H. (2021). Hierarchical pore structure based on cellulose nanofiber/melamine composite foam with enhanced sound absorption performance. Carbohydrate Polymers, 255, 117405.

[18]   Pulecchi, T., Manes, A., Lisignoli, M., & Giglio, M. (2010). Digital filtering of acceleration data acquired during the intervention of a lift safety gears. Measurement, 43(4), 455-468.

[19]   Boashash, B., & Mesbah, M. (2004). Signal enhancement by time-frequency peak filtering. IEEE Transactions on signal processing, 52(4), 929-937.

[20]   Xiang, L., & Yan, X. (2016). A self-adaptive time-frequency analysis method based on local mean decomposition and its application in defect diagnosis. Journal of Vibration and Control, 22(4), 1049-1061.

[21]   Xu, J., Wang, Z., Tan, C., Si, L., & Liu, X. (2017). A novel denoising method for an acoustic-based system through empirical mode decomposition and an improved fruit fly optimization algorithm. Applied Sciences, 7(3), 215.

[22]   Pedotti, L. A. D. S., Zago, R. M., & Fruett, F. (2017). Fault diagnostics in rotary machines through spectral vibration analysis using low-cost MEMS devices. IEEE Instrumentation & Measurement Magazine, 20(6), 39-44.

[23]   Miles, R. N. (2020). Physical Approach to Engineering Acoustics. Springer.

[24]   Zhou, J., & Miles, R. N. (2017). Sensing fluctuating airflow with spider silk. Proceedings of the National Academy of Sciences, 114(46), 12120-12125.

[25]   Zhou, J., Lai, J., Menda, G., Stafstrom, J. A., Miles, C. I., Hoy, R. R., & Miles, R. N. (2022). Outsourced hearing in an orb-weaving spider that uses its web as an auditory sensor. Proceedings of the National Academy of Sciences, 119(14), e2122789119.